

Real-Time 3D Ultrasound Guided Interventional System for Cardiac Stem Cell Therapy with Motion Compensation

Vijay Parthasarathy¹, Charles Hatt², Zoran Stankovic³,
Amish Raval², and Ameet Jain¹

¹ Philips Research North America, Briarcliff Manor, NY

² University of Wisconsin Medical School, Madison, WI

³ Philips Research Eindhoven, The Netherlands

Abstract. This paper describes a clinically translatable interventional guidance platform to improve the accuracy and precision of stem cell injections into a beating heart. The proposed platform overlays live position of an injection catheter onto a fusion of a pre-procedural MR roadmap with real-time 3D transesophageal echocardiography (TEE). Electromagnetic (EM) tracking is used to initialize the fusion. The fusion is intra-operatively compensated for respiratory motion using a novel algorithm that uses peri-operative full volume ultrasound images. Validation of the system on a moving heart phantom produced a landmark registration accuracy of $2.8 \pm 1.45\text{mm}$. Validation on animal *in vivo* data produced an average registration accuracy of $2.2 \pm 1.8\text{ mm}$; indicating that it is feasible to reliably and robustly fuse the MR road-map with catheter position using 3D ultrasound in a clinical setting.

Keywords: Stem cell therapy, Motion compensation, 3D TEE, EM tracking, Image fusion, Interventional cardiology.

1 Introduction

Stem cell repair of recently infarcted tissue could be a potential cure for patients with recent heart attacks [1]. One way to deliver stem cells to the infarcted region of a heart is through direct myocardial injection using a catheter. These cardiac injections need to be precisely targeted in order to avoid puncturing the infarcted portion; thereby needing precise localization of the catheter with respect to the anatomy of the heart that is moving due to both cardiac and respiratory motion. In this work, we aim to provide accurate localization by integrating three coordinate systems: 1) pre-operative MR road map, 2) live-3D ultrasound (US) using transesophageal echo, and 3) injection catheter. Such an interventional fusion system can help visualize the live 3D ultrasound volumes and the catheter in the larger context of the pre-procedural planning volumes. For this solution to be clinically viable in interventional cardiology and electrophysiology procedures, the set of registrations required to achieve this fusion needs to be accurate, fast, and robust, *i.e.* to be able to maintain continuous real-time registration between the different coordinate systems in free breathing mode for the entire procedure.

Maintaining continuous registration requires continuous re-adjustment of registration due to cardiac and respiratory motion. Continuous registrations of preoperative

volumetric images with real-time intraoperative ultrasound images are challenging and computationally demanding. In the case of real-time 3D ultrasound imaging probes like TEE and intracardiac echo (ICE), the accuracy and robustness of continuous registrations is compromised due to three factors: 1) small field-of-view (FOV) of ultrasound images, 2) artifacts and limited signal-to-noise ratio of *in vivo* ultrasound images, and 3) very different contrast mechanisms between pre-procedural images and ultrasound images.

Related Work. The demands of speed, accuracy, and robustness in procedures involving real-time registration have been addressed in several ways. Addressing the speed issue, Huang *et al.*, proposed using very small number of pixels along the edges of the image volumes for doing a mutual information based spatiotemporal registration [2]. This registration, however, was performed on data collected during breath-hold. Similarly, Sun et al [3], performed registration between 2D ICE and C-arm-CT volumes using cardiac and respiratory gating. To address the problem of different contrasts, King *et al.* [4] and Wein *et al.* [5] proposed a ultrasound physics-based simulation of the corresponding US image from the MR/CT volumes and used that to register with the live ultrasound images. Finally, in order to address the problem of small field of view of live ultrasound streams, Wein *et al.* [5] proposed using an extended field of view by sweeping the ICE catheter *in vivo* and reconstructing a larger field of view on-the-fly by constraining the catheter to lie on a linear trajectory model.

Contributions. In this paper, we develop an interventional guidance platform that includes a novel method to improve the accuracy and robustness of fusion between streaming live-3D ultrasound and pre-procedural MR images. An extended-FOV full-volume US image is used as an intermediary to register the live-3D ultrasound to the MR images. The large FOV of full-volume images and the similarity of contrasts and artifacts between full-volume US and live-3D ultrasound makes the proposed registration approach more robust, accurate, and efficient when compared to direct multimodal registration approaches. The interventional platform that integrates the proposed registration framework has been used and validated in three live animal experiments.

2 Methods and Materials

Clinical Workflow. Fig. 1 outlines the clinical workflow that was followed in using the proposed interventional guidance platform.

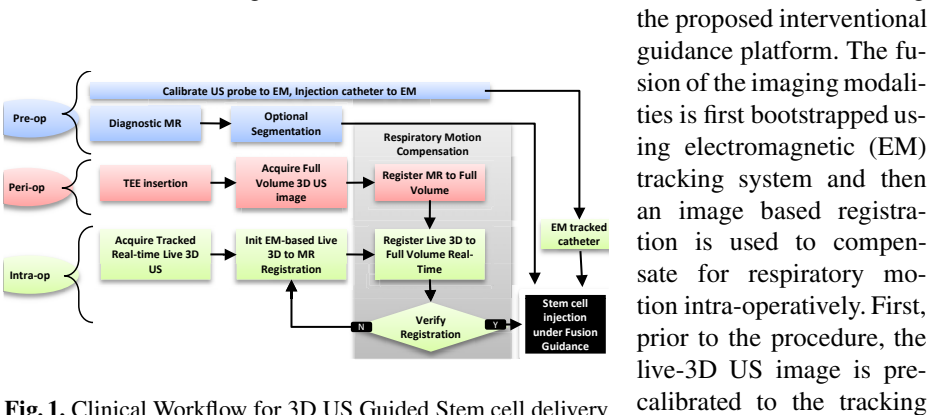


Fig. 1. Clinical Workflow for 3D US Guided Stem cell delivery

that was followed in using the proposed interventional guidance platform. The fusion of the imaging modalities is first bootstrapped using electromagnetic (EM) tracking system and then an image based registration is used to compensate for respiratory motion intra-operatively. First, prior to the procedure, the live-3D US image is pre-calibrated to the tracking

system by rigidly attaching 6-DOF EM sensors to the probe and calibrating using the method described in [6]. Second, the tip of the stem cell injection catheter is also pre-calibrated to the 5-DOF EM sensor mounted on it. During the procedure, pre-operative MR images are acquired with cardiac and respiratory gating. The specific MR volume that is used to segment the infarct is acquired at end-expiration and at a particular cardiac phase in diastole. In this work, we call that phase the ‘infarct phase’, which is determined by the MR imaging parameters. MR images are acquired with external fiducials stuck on the subject’s body that are used for MR-EM registration. The injection targets are usually planned on the border zone between the infarct and healthy heart tissue.

During the procedure, a 6-degree of freedom (DOF) EM tracking sensor is rigidly mounted to the patient table and acts as a ground reference for the tracking system. MR images are registered to the EM frame of reference using fiducials. Following the MR-EM registration, TEE ultrasound probe is inserted into the esophagus. Live-3D ultrasound images are streamed live into the fusion workstation, wherein the fusion between MR and L3DUS is initialized using EM tracking. This initial registration is valid only at end-expiration and the ‘infarct phase’.

The stem cell injection procedure, however, is performed in free breathing mode, during which the motion compensation algorithm is used to correct the registration for respiratory motion at every ‘infarct’ phase. In order to perform the motion compensation, an one time acquisition of full-volume 3D ultrasound volume is acquired using ECG gating at end-expiration. The MR images and the full-volume 3D US are registered using visual assessment. During the stem cell injection procedure, the live-3D US images are registered to the MR images using the full-volume 3D US using the algorithms described below. In addition, the EM tracked position of the injection catheter is displayed live within the motion compensated MR volume. Any gross motion of the US probe is also tracked, thereby providing continuous and robust tracking of the live-3D US volume in a motion compensated MR volume. The quality of the registration is monitored visually by the interventional cardiologist, and in the event of drift in registration, the registration is re-initialized using the EM based framework.

Real-time Respiratory Motion Compensation. The full-volume ultrasound (FVUS) is used as an intermediary in the registration between live-3D ultrasound (L3DUS) and MRI. Mathematically, ${}^{\text{MR}}\mathbf{T}_{\text{L3DUS}} = {}^{\text{MR}}\mathbf{T}_{\text{FVUS}} \bullet {}^{\text{FVUS}}\mathbf{T}_{\text{L3DUS}}$. The acquisition of full-volume ultrasound volumes is a feature that already exists in the Philips xMatrix™ probes (Philips Healthcare, Bothell, WA). Full-volume imaging is an ECG gated acquisition of the 3D+Time volumetric acquisition of the entire heart in four heart beats. The ‘infarct phase’ in the full-volume image is identified using QLAB image analysis tool (Philips Healthcare, Bothell, WA) using the ECG gating values, and is manually registered to the MR image volume to yield a rigid transformation ${}^{\text{MR}}\mathbf{T}_{\text{FVUS}}$. The ‘infarct phase’ of the live 3D ultrasound stream is determined using a time-synchronized ECG gating signal that is output from the Ultrasound scanner via a dedicated A/D card (National Instruments, Austin, TX). Both the live-3D and the full-volume images are scan converted before registration.

Since the registration is performed only during the ‘infarct phase’ of the cardiac cycle, we use a rigid transformation to register the two ultrasound volumes. Mutual information (MI) is used as similarity metric in the registration [2]. A thresholding step

is performed on the ultrasound images prior to the mutual information computation to consider voxels only in areas with non-zero signal. The registration problem is framed as an optimization problem, $\arg \max_{\phi} \text{MI}(\text{L3DUS}, \text{FVUS} \circ \mathbf{T}(\phi))$ where ϕ is a 6 parameter rigid transform vector parameterizing the rigid homogenous transformation matrix (${}^{\text{L3DUS}}\mathbf{T}_{\text{FVUS}}$) between full-volume ultrasound and live-3D ultrasound. The registration was implemented in an ITK framework [7]. A regular step size gradient descent optimizer was used for the optimization. The algorithm is integrated within the visualization platform with several user interfaces to control the optimizer behavior and the similarity metric computation, especially the number of histogram samples.

3 Experimental Design and Results

3.1 Phantom Validation

We conducted three phantom-based validation experiments to 1) validate the accuracy of EM-tracking based initialization, 2) measure the landmark registration accuracy, and 3) validate the motion tracking accuracy.

Accuracy of EM-Based Initialization. The accuracy of the EM based initialization was computed on a stationary heart phantom, which is a replica of a human heart, built in-house and constructed using poly-vinyl alcohol and doped to provide realistic visibility in both MR and ultrasound. The one time calibration of the live 3D US image coordinate to the 6-DOF EM sensor was performed with a calibration accuracy of 1.94 mm [6]. MRI images of the phantom were acquired using Philips Panorama 1T system with fiducials mounted on the phantom. The fiducials were used to register the MR to the EM frame of reference by localizing them in both coordinate systems. This approach resulted in a fiducial registration error (FRE) of 1.29 mm and target registration error (TRE) of 1.77 mm. It was also observed that keeping the fiducials too far apart decreased the accuracy due to EM distortions. Further, in order to measure US-MR fusion accuracy, seven home made thread-like fiducials were attached to the surface of the heart phantom. These were visible on both MRI and on 3D US images. By manually segmenting them in the 3D US and MRI images, and comparing the transformed points to the ones segmented in MRI, we estimated the US-MRI registration accuracy with a mean landmark accuracy 3.3 ± 0.22 mm.

Registration Accuracy Using Respiratory Motion Phantom. For the next two phantom validation studies, we designed a servomechanisms to move the heart phantom on a ramp to simulate respiratory motion (see Fig. 2). In addition, a new ‘apex’ was designed as a detachable slab that can fit custom made target samples to measure landmark accuracy. These samples are 4.5 mm in radius and are doped with magnevist and graphite to achieve realistic contrast in both MR and in ultrasound.

Image acquisition: An IE33 ultrasound scanner with X7-2T TEE probe (Philips Healthcare, Bothell, WA) was used to acquire both the full-volume and streaming ultrasound data sets. The pre-procedure MR was acquired on a GE 1.5T MR scanner (GE Healthcare, Waukesha, WI).

Experiments: The respiratory motion ramp had both translation and rotation stages. Ground truth motion was tracked using a dedicated 6-DOF EM sensor attached to the moving stage. The phantom was moved to three positions on the ramp at approximately 5, 10, and 15 mm from the baseline position; displacements that are representative of the amount of respiratory motion that we expect in a clinical setting [8]. At each position, three trials of the proposed registration was performed with the baseline registration being loaded before every trial. The full-volume based registration was performed using 1.6% of the number of pixels in the live-3D ultrasound image for histogram computation. The pixels were randomly sampled at each iteration of the registration. The amount of motion computed using the full-volume based registration was compared against the ground truth from the reference EM sensor. On an average from all trials and all positions, the translation error was 2.25 ± 1.96 mm and rotation error was 4.5 ± 1.98 degrees.

Landmark Accuracy Using Respiratory Motion Phantom.

Another validation study was performed with the same phantom experimental set-up as described in the previous study. In this study, eight custom made fiducials were segmented from the MR images and the center of these segmentations were marked as targets. At each displacement of the phantom, three trials of full-volume US based registration was performed and the fusion between MR and live 3D was visualized. The centers of the fiducials were manually segmented from the US volumes (with MR visualization switched off to avoid bias) and transformed to the MR coordinate frame using the computed registration. These co-ordinates were then compared to the fiducials segmented in the MR coordinate frame. Since the FOV of the live-3D volumes is limited, only 3 fiducials were visible for computing landmark error. The average landmark registration error was 2.8 ± 1.45 mm.



Fig. 2. Custom built heart phantom with multi-modality visibility employed for in vitro experiments, and screen shot of MR-US fusion

3.2 Animal Data Validation

We are currently evaluating the accuracy and robustness of the proposed fusion system in series of animal studies. In this paper, we present data from three anesthetized pigs with acute myocardial infarction that was created 2-4 days prior to the procedure. All studies were performed within the guidelines set by the Committee of Animal Research and Ethics at the University of Wisconsin Hospital, Madison, WI.

Image Acquisition: The baseline MR images were collected using the delayed hyper-enhancement MR protocol at breath-hold. The MR volumes are $256 \times 256 \times 20$ with a resolution of $1.3 \times 1.3 \times 5$ mm. Following the MR imaging, the pig is brought to the cath-lab where the TEE probe is inserted and full volume US images are acquired at breath-hold and end-expiration. After scan conversion, the size of the full-volume images are $224 \times 208 \times 208$ with a pixel resolution of $0.5 \times 0.5 \times 0.48$ mm. The live 3D images are streamed in real-time to the workstation at ≈ 20 Hz with a size of $112 \times 48 \times 112$ with a pixel spacing of $0.7827 \times 0.9403 \times 0.9229$ mm.

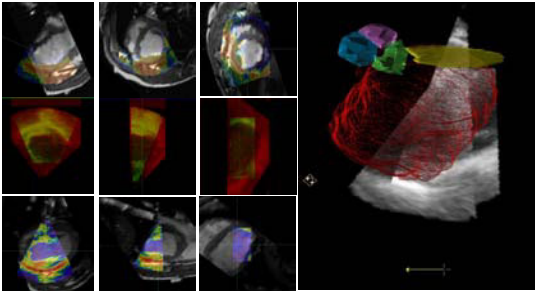


Fig. 3. Left: Top Row shows fusion of full-volume US and MR images, middle row shows results of intra-operative registration of live-3D US and full-volume US, bottom row shows fusion between live-3D and MR that is shown to the user. Right: 3D visualization of 2 multi-planar reformats (MPR) of the Live-3D ultrasound volume with the segmented MR images displayed as a mesh with aortic (yellow) and mitral valve leaflets also segmented to provide 3D context. The catheter is displayed as a yellow arrow seen in the bottom

The minimum number of histogram samples needed to achieve as stable registration varied between 1250 (0.06% of US image size) samples to 10000 samples (1.6% of US image size) depending on the amount of high-frequency details on the ultrasound images. The histogram parameters could be changed dynamically by the user during the procedure depending on the robustness of the registration. The time for registration varied between 350 milliseconds for 1250 to 3 seconds for 10000 samples on a 2.66GHz Dual Quad-Core processor with 4GB DDR memory. Example of a qualitative evaluation of the registration can be seen in Fig. 3, which

shows good overlap between live-3D US and MR images in 2D and 3D visualizations.

***In vivo* Motion Compensation Accuracy.** One live-3D ultrasound image corresponding to the ‘infarct phase’ was selected manually from the live-3D US stream and analyzed off line. The ground truth registration between this live-3D image and the full-volume US image was selected manually with expert physician’s guidance. Five hundred registration trials were performed, with initializations randomly misaligned around the ground truth registration with uniform distribution. For the capture range experiments, the translation and rotations were simultaneously varied by 15 mm and 15 degrees respectively with a uniform distribution. Similarly, for the accuracy related experiments, the translation and rotation shifts were simultaneously varied by 9 mm and 9 degrees respectively. The capture range was defined as the error below which >90% of the misalignments were able converge to an error < 3 mm. The number of histogram samples was set at 1.6% of image size of live-3D US. From data analyzed from 3 pig data sets, the average translation error compared to ground truth was 1.5 ± 1.7 mm, and rotation error was 4.9 ± 3.9 degrees, with overall registration accuracy of 2.2 ± 1.8 mm. These average values of accuracy and robustness to randomly varying initializations is indicative of the smoothness of the objective function between full-volume US and live-3D US. The average capture range for the algorithm was 15.3 ± 2.1 mm, which is greater than respiratory motion in humans [8].

***In vivo* Validation of Respiratory Motion Tracking.** Managing synchronization [9] and data frame rates of streaming data – ECG, ultrasound and EM — is a challenge

in interventional systems such as the one proposed in this paper. In order to test the proposed motion compensation system on reduced data rates, we tested its robustness to sub-sampling of US image streams in spatial and temporal dimensions. We established ground truth data by using a cardiac-gated 15 second long sequence high-resolution

live-3D images acquired at 30 Hz (444 images in sequence) on the IE33 on free-breathing pig. The breathing rate was set at 17 breaths/min on the ventilator and the cardiac rate was 81 beats/min. Each frame was rigidly registered to the full volume ‘infarct phase’ in a sequential manner with the registration results from image n serving as an initialization to registration to image $n + 1$. Although the deformation between the full volume and live-3D is indeed non-rigid, a rigid registration transform is used to approximate the translation and rotation offset between the two images. The first initialization was done manually.

Data shown in Figs. 4(a) and (c) represents the computed rotation and translation motion of the heart that is used as the ground truth for this study. Figs. 4(b) and (d) show the respective sinusoidal components extracted using Fourier analysis of the motion tracking data. The blue curves are the measured rotation and translation values

shown with mean subtracted for clarity of visualization. The red curves in these plots are samples of the tracking values at R-wave ECG trigger; and hence should ideally represent only respiratory component of cardiac motion. Note that the number of cardiac and respiratory cycles correlate with the cardiac and respiratory rate of the animal.

The stream of 444 images was sub-sampled in both spatial and temporal directions and the sequential registrations were performed on these sequences. The result was compared to the ground truth. Results in Table 1 show that the motion compensation is very robust to temporal

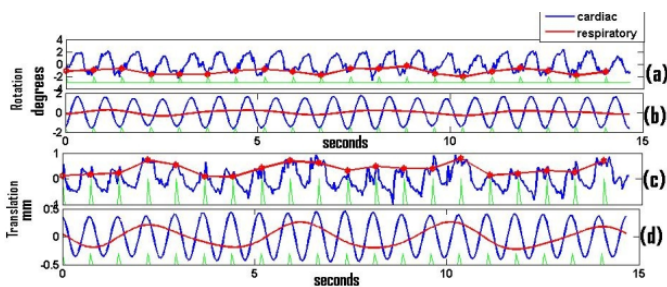


Fig. 4. Results of the motion compensation algorithm. Rotation and translation tracking of the cardiorespiratory motion of the heart respectively can be seen in (a) and (c) respectively. (b) and (d) show the underlying sinusoidal motion components of cardiac (blue) and respiratory (red) motion components

Table 1. Robustness to spatial and temporal decimation of live 3D streams

Temporal sub-sampling		
Freq(Hz)	Rot err(deg)	Trans err(mm)
15	0.23	0.12
10	0.23	0.08
6	0.20	0.08
3	0.34	0.15
Spatial sub-sampling		
Pix size red(%)	Rot err(deg)	Trans err(mm)
20	1.3	0.37
60	1.73	0.40
100	0.69	0.37
200	1.15	0.52

decimation of the streams with errors < 1 mm even for 3 Hz temporal acquisitions. In addition, the reduction of spatial resolution by 200% yields an error on only about 1.15 degrees and 0.52 mm suggesting that the algorithm is robust to sub-sampling in both spatial and temporal resolutions.

4 Discussion and Conclusion

A clinically translatable multi-modality fusion system for stem cell therapy has been proposed. The system integrates a novel motion compensation scheme that uses full-volume ultrasound imaging to enhance the accuracy, robustness, and speed of fusion between MRI and live-3D ultrasound. Validation on a moving heart phantom and preliminary data from animal studies have demonstrated the clinical feasibility of the proposed approach. Further *in vivo* validation of respiratory motion tracking and management of latencies in the system will be crucial to translate this technology to human clinical studies. Prospective registration schemes for respiratory motion compensation is another research direction to make this technology work in real-time.

References

1. Wollert, K., Drexler, H.: Does cell therapy work for myocardial infarction and heart failure work? *Dialogues in Cardiovascular Medicine* 14(1), 37–43 (2009)
2. Huang, X., Ren, J., Guiraudon, G., Boughner, D., Peters, T.M.: Rapid dynamic image registration of the beating heart for diagnosis and surgical navigation. *IEEE Transactions on Medical Imaging* 28(11), 1802–1814 (2009)
3. Sun, Y., Kadoury, S., Li, Y., John, M., Resnick, J., Plambeck, G., Liao, R., Sauer, F., Xu, C.: Image guidance of intracardiac ultrasound with fusion of pre-operative images. In: Ayache, N., Ourselin, S., Maeder, A. (eds.) *MICCAI 2007, Part I*. LNCS, vol. 4791, pp. 60–67. Springer, Heidelberg (2007)
4. King, A.P., Ma, Y.-L., Yao, C., Jansen, C., Razavi, R., Rhode, K.S., Penney, G.P.: Image-to-physical registration for image-guided interventions using 3-D ultrasound and an ultrasound imaging model. In: Prince, J.L., Pham, D.L., Myers, K.J. (eds.) *IPMI 2009*. LNCS, vol. 5636, pp. 188–201. Springer, Heidelberg (2009)
5. Wein, W., Camus, E., John, M., Diallo, M., Duong, C., Al-Ahmad, A., Fahrig, R., Khamene, A., Xu, C.: Towards Guidance of Electrophysiological Procedures with Real-Time 3D Intracardiac Echocardiography Fusion to C-arm CT. In: Yang, G.-Z., Hawkes, D., Rueckert, D., Noble, A., Taylor, C. (eds.) *MICCAI 2009*. LNCS, vol. 5761, pp. 9–16. Springer, Heidelberg (2009)
6. Lang, A., Parthasarathy, V., Jain, A.: Calibration of 3D Ultrasound to an Electromagnetic tracking system. In: D’hooge, J., Doyley, M.M. (eds.) *Proceedings of the SPIE Medical Imaging 2011: Image Guided Procedures*. SPIE, vol. 7968 (2011)
7. Ibanez, L., Schroeder, W., Ng, L., Cates, J.: *The ITK Software Guide*, 2nd edn (2005)
8. Shechter, G., Ozturk, C., Resar, J.R., McVeigh, E.R.: Respiratory motion of the heart from free breathing coronary angiograms. *IEEE Trans. Med. Im.* 23(8), 1046–1056 (2004)
9. Sundar, H., Khamene, A., Yatziv, L., Xu, C.: Automatic image-based cardiac and respiratory cycle synchronization and gating of image sequences. In: Yang, G.-Z., Hawkes, D., Rueckert, D., Noble, A., Taylor, C. (eds.) *MICCAI 2009*. LNCS, vol. 5762, pp. 381–388. Springer, Heidelberg (2009)